UNIVERSITEIT
AMSTERDAM

VU Research Portal

Predicting the influence of hip and lumbar flexibility on lifting motions using optimal control

Sreenivasa, Manish; Millard, Matthew; Kingma, Idsart; van Dieën, Jaap H.; Mombaur, Katja

Link to publication in VU Research Portal

Predicting the influence of hip and lumbar flexibility on lifting motions using optimal control

Manish Sreenivasa [a,b,*], Matthew Millard [b], Idsart Kingma [c], Jaap H. van Dieën [c], Katja Mombaur [b]

[a] School of Mechanical, Materials, Mechatronic & Biomedical Engineering, University of Wollongong, NSW 2522, Australia
[b] Optimization, Robotics & Biomechanics, Institute of Computer Engineering, Heidelberg University, Germany
[c] Department of Human Movement Sciences, Faculty of Behavioural and Movement Sciences, Vrije Universiteit Amsterdam, Amsterdam Movement Sciences, Amsterdam, The Netherlands

ARTICLE INFO

ABSTRACT

Computational models of the human body coupled with optimization can be used to predict the influence of variables that cannot be experimentally manipulated. Here, we present a study that predicts the motion of the human body while lifting a box, as a function of flexibility of the hip and lumbar joints in the sagittal plane. We modeled the human body in the sagittal plane with joints actuated by pairs of agonist-antagonist muscle torque generators, and a passive hamstring muscle. The characteristics of a stiff, average and flexible person were represented by co-varying the lumbar range-of-motion, lumbar passive extensor-torque and the hamstring passive muscle-force. We used optimal control to solve for motions that simulated lifting a 10 kg box from a 0.3 m height. The solution minimized the total sum of the normalized squared active and passive muscle torques and the normalized passive hamstring muscle forces, over the duration of the motion. The predicted motion of the average lifter agreed well with experimental data in the literature. The change in model flexibility affected the predicted joint angles, with the stiffer models flexing more at the hip and knee, and less at the lumbar joint, to complete the lift. Stiffer models produced similar passive lumbar torque and higher hamstring muscle force components than the more flexible models. The variation between the motion characteristics of the models suggest that flexibility may play an important role in determining lifting technique.

© 2018 Published by Elsevier Ltd.

1. Introduction

Mechanics-based models can represent the human body as articulated segments that describe the general movement of the limbs. Coupled with computational methods such models prove useful in investigating human movement parameters that may be difficult to directly measure, such as joint torques. We identify two general approaches to such investigations; First, by using experimental data to estimate what the human was doing (inverse-methods), such as (Faber et al., 2011; Kingma et al., 2004). Second, by simulating or predicting novel control signals, and computing the corresponding movements and internal physiological states (Burg et al., 2005; Arjmand and Shirazi-Adl, 2006; Dreischarf et al., 2016; Millard et al., 2017). Predictive simulations are computationally intensive and require methods, such as optimal control (OC), to generate the control signals specific to various movement tasks. In general, optimal control solves for state and control trajectories that satisfy the system dynamics subject to constraints such that the value of an underlying objective function is minimized. More commonly, optimal control has been applied to simulating gait (Anderson and Pandy, 2001; Ackermann and van den Bogert, 2010; Mombaur, 2016; Sreenivasa et al., 2017) and sit-to-stand motions (Sadeghi et al., 2013; Mombaur and Hoang, 2017), with relatively limited number of studies focusing on lifting motions (Arjmand and Shirazi-Adl, 2006; Manns et al., 2017; Millard et al., 2017; Harant et al., 2017). Despite these challenges, simulations can help answer biomechanical questions that are impractical or impossible to answer using experimental analysis alone. Examples of such questions are those that study the effect of varying muscle strength (Steele et al., 2012), or the effect of orthosis stiffness on patient gait (Sreenivasa et al., 2017), or the influence of varying cost function (Arjmand and Shirazi-Adl, 2006; Sadeghi et al., 2013; Mombaur and Hoang, 2017).

The biomechanics of lifting motions are of particular interest as they require the coordination of muscles over the whole body involving concentrated loads over several joints. As a common

* Corresponding author at: School of Mechanical, Materials, Mechatronic & Biomedical Engineering, University of Wollongong, NSW 2522, Australia.
E-mail address: manishs@uow.edu.au (M. Sreenivasa).

daily activity, excessive cumulative lower back loads (CLBL) during lifting, computed as the integral of net back moments over time, have been associated with risk of injury and lower-back pain (Coenen et al., 2013). Physiological factors, as well as the lifting configuration and speed, can affect the characteristics of an individual's lifting motion and the load on the lower back (Faber et al., 2011; Kingma et al., 2004; Buseck et al., 1987). However, there remains a gap in our understanding of the relationship between an individual's flexibility and their lifting motion. Note that for the purpose of this study we use the term flexibility to denote a combination of kinematic and kinetic characteristics of the movement about a joint. For example, the musculature around a less flexible joint would generate higher passive torques at a given range of motion (ROM) when compared to a more flexible joint. Previous studies have reported on the lumbar (Dolan et al., 1994) and hip (Gajdosik et al., 1994) ROM, but do not investigate the influence of limited ROM on the whole body movement. From an experimental point-of-view, finding a population of subjects with suitable range of flexibility and having an objective comparison between their lifting styles is a difficult endeavor.

The goal of this study was to use simulations to investigate the influence that hip and lumbar flexibility can have on the kinematics and dynamics of lifting motions. In this context, we developed a model of the human body and formulated an optimal control problem (OCP) for predicting lifting motions. Model flexibility was modified to simulate a stiff, average and flexible person, in order to answer the question - How does the predicted model motion change with flexibility? This study was conducted in the context of wearable robots (exoskeletons) that work in close coupling with the human body. An additional focus was on the inferences that we may make from our results towards the design of such exoskeletons.

2. Materials and methods

2.1. Human models

We modeled the human body in the sagittal plane and combined the left and right limbs. This was done to reduce model complexity and under the focus of evaluating left-right symmetric motion that occurs primarily in the sagittal plane. The model consisted of an articulated multibody system with 10 segments (Fig. 1). The pelvis segment was modeled as a floating base with two translational and one rotational degrees of freedom (DoF). All other segments were modeled with one rotational DoF each, to give a total of 12 DoF. The human model's segment lengths corresponded to those recorded from a 35-year old male (1.74 m in height, 81.0 kg in weight). Segment mass and inertia properties were first approximated from anatomical regression equations (de Leva, 1996) using the subject's height and weight. The ratio of the subject-specific segment lengths to the default lengths provided by de Leva (1996) were then used to linearly scale the segment mass and inertia, using the model creation software ModelFactory (Sreenivasa and Harant, 2018).

All internal DoFs were actuated by pairs of agonist-antagonist muscle torque generators (MTG) (Millard et al., 2017). Each MTG represented the torques generated by the active (τ^A) and passive (τ^P) muscle components in one rotational direction as,

$$\tau = \tau^A + \tau^P \quad \text{with,} \tag{1}$$

$$\tau^A = \tau_o a \mathbf{f}^A(\theta) \mathbf{f}^V(\omega) \tag{2}$$

$$\tau^P = \tau_o \mathbf{f}^{PE}(\theta)\left(1 - \beta^{PE}\frac{\omega}{\omega_{\max}^M}\right) \tag{3}$$
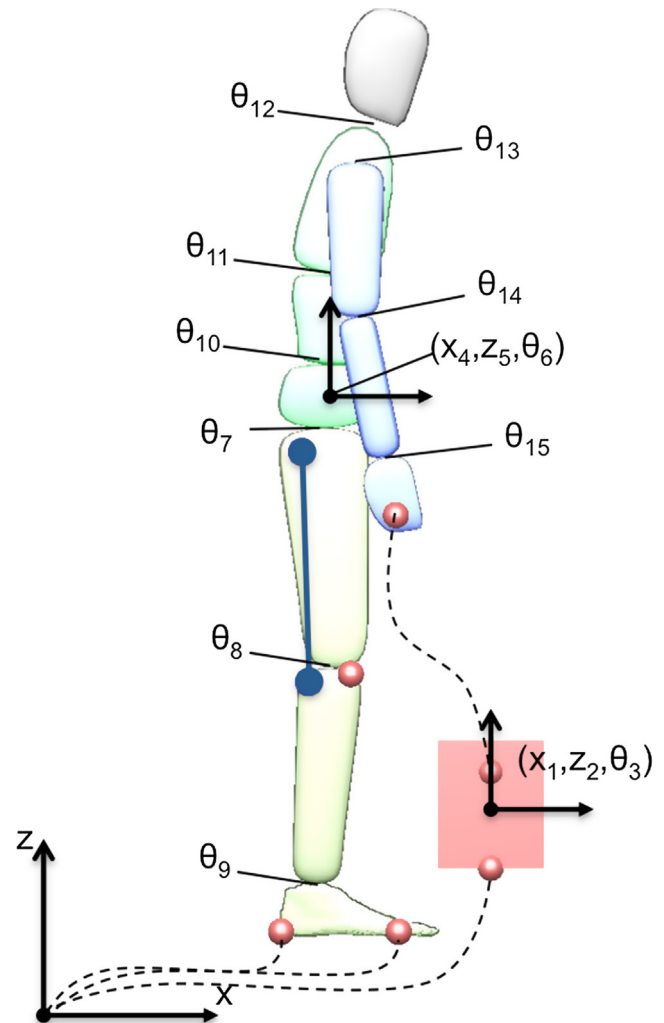

Fig. 1. A sagittal plane human model was used to simulate the motions while lifting a 10 kg box. Illustrated are the human and box degrees of freedom. A line-type passive hamstring muscle is illustrated as a blue line extending from the pelvis to the shank segment. Dashed lines indicate kinematic constraints imposed during the motion between points on the feet and the floor, and the box and the hands. (For interpretation of the references to colour in this figure legend, the reader is referred to the web version of this article.)

where θ were the joint angles, ω were the joint angular velocities, τ_o was the maximum isometric torque, a was the muscle activation, $\mathbf{f}^A(\theta)$ was the value from the active torque-angle curve, $\mathbf{f}^V(\omega)$ was the value from the torque-velocity curve, $\mathbf{f}^{PE}(\theta)$ was the value from the passive-torque-angle curve, and, β^{PE} was a normalized damping coefficient. We chose to use MTGs in this study in favor of line-type muscles (e.g. Christophy et al., 2012; van Dieën and Kingma, 2005) as we were interested in the overall coordination of the limbs rather than in the bone-on-bone contact forces. The relative simplicity of the MTGs also helps reduce the complexity of the optimal control problem. We also note that lumbar disk compressive forces have been found to be highly correlated with net moments about the L5/S1 vertebra (van Dieën and Kingma, 2005), allowing simpler models such as the one used in this study to be useful in estimating loading on the vertebral disk.

A total of 18 MTGs produce flexion-extension torques that actuated the segments. We added damping at the model's joints that represents the passive damping arising from the musculature and tissue surrounding the joint. Most of the passive and active muscle properties were identical to the model defined in Millard et al.

(2017). The exceptions were the passive torques of the lumbar extensor, hip extensor and the knee flexor, as detailed further. An open-source implementation of the MTGs is available as an addon in the rigid-body dynamics library RBDL (https://rbdl.bitbucket.io).

2.1.1. Passive muscle properties

We modified the contributions from passive muscle components to reflect a stiff, average, and flexible person. We limit the lumbar range-of-motion (RoM) in flexion and modify the passive extension torque generated by the lumbar-extensor MTG.

Dolan et al. measured the lumbar flexion RoM in healthy adult males and reported an average of 53.3° with a range from 38.5° to 69.4° (Dolan et al., 1994). The study also reported an average peak passive lumbar extensor torque of 84.0Nm across all subjects at 97.3% of peak flexion angle. We used Dolan's findings to model a stiff, average and flexible lumbar extensor that generates 84.0Nm of passive lumbar extension torque at 37.4°, 51.8° and 67.5° of lumbar flexion angle, respectively (note that these angles differ from the mean and range reported in Dolan et al. as they refer to the point of the curve where 84.0Nm is developed, which is slightly less than at 100% flexion). The passive force-length curve of the lumbar extensor was adjusted such that the normalized-force-length remained constant and the MTG generated the required extension torque at the desired lumbar flexion angle. This modification is consistent with an optimal fiber length that is shortened to make a muscle stiffer and lengthened to make it more flexible.

We modeled the passive contribution of the bi-articular hamstrings by including a line-type muscle spanning the pelvis, hip and knee joints (Fig. 1). We chose to model the hamstring muscle and only its passive component based on literature evidence on the important role played by the hamstring during bending and lifting tasks, especially in the coordination of the pelvis, hip and knee (Gajdosik et al., 1994; Kang et al., 2013). The muscle origin point on the pelvis segment and insertion point on the shank segment were modeled as per (Brand et al., 1982). The passive force of the hamstring, f_{ham}, was applied to the origin and insertion points on the model, and computed as,

$$f_{ham} = f_o f^{PE}(\tilde{l})(1 + \beta \tilde{v}) \tag{4}$$

where $f_o = 4696.0$ N was the maximum isometric force as per (Hoy et al., 1990). Note that here we have doubled the value of f_o to account for our sagittal plane model that combines the right and left limbs. $f^{PE}(\tilde{l})$ was the normalized force-length curve as per (Millard et al., 2013). $\tilde{l}$ was the normalized muscle length and calculated as,

$$\tilde{l} = \frac{l - lt_{slack}}{l_{opt}} \tag{5}$$

where l was the current muscle length, $lt_{slack} = 0.385$ m and $l_{opt} = 0.107$ m were the tendon slack length and optimal fiber length as per (Hoy et al., 1990). β was a damping term set to 0.1 and $\tilde{v}$ was the normalized muscle velocity. We assumed a rigid tendon and a pennation angle of zero.

Gajdosik et al. measured the flexibility in hip flexion across 30 young men during a toe-touch task with the knees straightened (Gajdosik et al., 1994). Subjects were classified with short, medium and long hamstrings as being able to reach hip flexion angles of 59.0°, 68.7° and 76.7°, respectively. We modeled the characteristics of a stiff, average and flexible hip such that the hamstring muscle produced 129.4Nm of extension torque at the flexion RoM corresponding to a short, medium and long hamstring. This value of extension torque was estimated from inverse-dynamics analysis of a toe-touch motion of a subject of similar height and weight as our model (Millard et al., 2017). Hamstring flexibility was modulated by solving for the new optimal fiber length, l_{opt}, such that the hamstring muscle developed the desired passive extension

torque at the hip joint at the desired hip flexion angle (with straightened knee).

Note that the passive components, but not the active components, of the hip extensor and knee flexor MTGs were turned off, as these passive forces were now provided by the passive hamstring muscle. The lumbar passive extensor and hamstring characteristics were co-varied to create 3 model variations corresponding to a stiff-lifter, an average-lifter and a flexible-lifter (see Table 1 for summary). The motivation behind co-varying the hip and lumbar flexibility was evidence that short hamstrings in a person is associated with decreased lumbar RoM (Gajdosik et al., 1994).

2.1.2. Activation dynamics

MTG activation was computed using first-order activation dynamics,

$$\dot{a} = \frac{e - a}{t_{ad}} \tag{6}$$

where $\dot{a}$ was the rate of change in activation, e represents the muscle excitation signal, and t_{ad} the activation-deactivation time constant (Thelen, 2003). We set $t_{ad} = 50$ ms for the MTGs of the shoulder, elbow, hand and head, which is equal to the deactivation time constant reported by Thelen (2003). Note that unlike (Thelen, 2003), we assumed the same time constants for activation and deactivation in order to have a continuous function for $\dot{a}$. For the MTGs of the hip, knee, ankle and lumbar joints, we derived the time constants from recordings of the electromechanical delay (EMD) reported in literature (Table 2). This was motivated by our observation that the nominal value of $t_{ad} = 50$ ms was too fast for the bigger muscles, such as those at the back and hip. We assumed that the tasks in the EMD literature have a dominant frequency of 1 Hz, allowing us to map the EMD delay to a phase shift, and finally to t_{ad} in Eq. (6).

2.2. Optimal lifting motions

We used a multiple shooting method described by Bock and Pitt (1984) and implemented in the software MUSCOD-II (Leineweber et al., 2003) to solve for optimal lifting motions. The dynamical system solved by the method refers to the equations of motions governing the MTG actuated multi-body human model. The details of the OCP setup and numerical method are identical to that in Millard et al. (2017). Here, we summarize the salient points of the OCP relevant to the prediction of lifting motions.

The lifting motion was defined as 3 phases; bending, gripping and lifting (Fig. 2). The constraints between the hands and the box change across phases which also changes the underlying dynamics. The objective function was defined as,

$$\min_{x(\cdot), e(\cdot), v} \sum_{j=1}^{3} \int_{v_j}^{v_{j+1}} \left[\sum_{k=0}^{n_k} \left\{ \frac{(\tau_k^A)^2}{(\tau_o)_k^2} + \frac{(\tau_k^P)^2}{(\tau_o)_k^2} + \delta e_k^2 \right\} + \left(\frac{f_{ham}}{f_o} \right)^2 \right] dt \tag{7}$$

Table 1
Flexibility characteristics of the hip and lumbar joints for the stiff, average and flexible models. The indices specify the relevant joints (see Fig. 1). The values indicate the target flexion angles and corresponding extension torques used for fitting the lumbar extensor MTG's and hamstring muscle's passive properties. The values for the hip are with straight knees and only relate to hamstrings tension; with knee flexion this value increases based on hamstring length.

		Model Type		
		Stiff	Average	Flexible
Hip	θ_7	59.0°	68.7°	76.7°
	τ_7^P		129.4 Nm	
Lumbar	$(\theta_{10}, \theta_{11})$	37.4°	51.8°	67.5°
	$(\tau_{10}^P, \tau_{11}^P)$		84.0 Nm	

where $\mathbf{x}(\cdot) = [\theta\ \omega\ a]$ was a vector of state variables, e_k were the control inputs for the simulation (neural excitations, Eq. (6)), $j = 1, \ldots, 3$ iterates through the motion phases which begin at time v_j and end at v_{j+1}, and $k = 0, \ldots, n_k$ iterates over the MTGs. The term δe_k^2 was a regularization term that introduced a small cost to the objective function value and served to smoothen the control inputs. We set δ to 0.1 for our simulations.

Note that this objective function minimizes the passive and active torques over all MTGs of the model and not just those at the lower back. This is in contrast to studies in ergonomics, e.g. Arjmand and Shirazi-Adl (2006) and van Dieën and Kingma (2005), where mainly lumbar forces/torques are minimized. In the present study, we were interested in simulating movement of the whole body and only minimizing the lumbar torques would not have been sufficient for this goal. It is important to note that in contrast to Arjmand and Shirazi-Adl (2006) and van Dieën and Kingma (2005), in this study we were computing a forward simulation that predicted motion kinematics as well as kinetics. To the best of our knowledge, objective functions used in ergonomics literature are typically used to solve for muscle forces under known kinematics and kinetics, and hence a direct comparison to this study is not possible. Forward simulations using objective functions are relatively more commonly used in the simulation of walking and running.

A typically used objective function is one that minimizes the integral over time of the muscle activations raised to a power (Ackermann and van den Bogert, 2010), although other formulations have also been proposed (Mombaur, 2016, Afschrift et al., 2016, Serrancolí et al., 2017, Sadeghi et al., 2013, Mombaur and Hoang, 2017).

The motivation behind our formulation was to include the influence of passive muscle components in our simulations, as opposed to objective functions that are based on muscle activation and therefore only take active components into account. Note that our objective function contains the active and passive components separately, and not as the net MTG torque. This was motivated by our observation that the formulation based on net MTG torques did not adequately consider passive muscle components, leading to movements with unnaturally large passive forces. There is evidence that repeated stretching of spinous ligaments may lead to back injury (Solomonow et al., 2003). It is plausible that a human might shape their movements to avoid high muscle forces, because humans have sensors to provide muscle force information via golgi-tendon organs. In the following, we describe the main constraints that were applied during the motion.

1. *Bending* - The bending phase started with the human model standing upright and still, with a 10 kg box placed in front (Fig. 2).

Table 2
Activation-Deactivation time constants, t_{ad} (Eq. (6)), derived from reported values of electromechanical delay (EMD). t_{ad} for the head, shoulder, elbows and hands were set to 50 ms. The values indicated refer to the time constants and EMD associated with the major muscle driving motion in that direction.

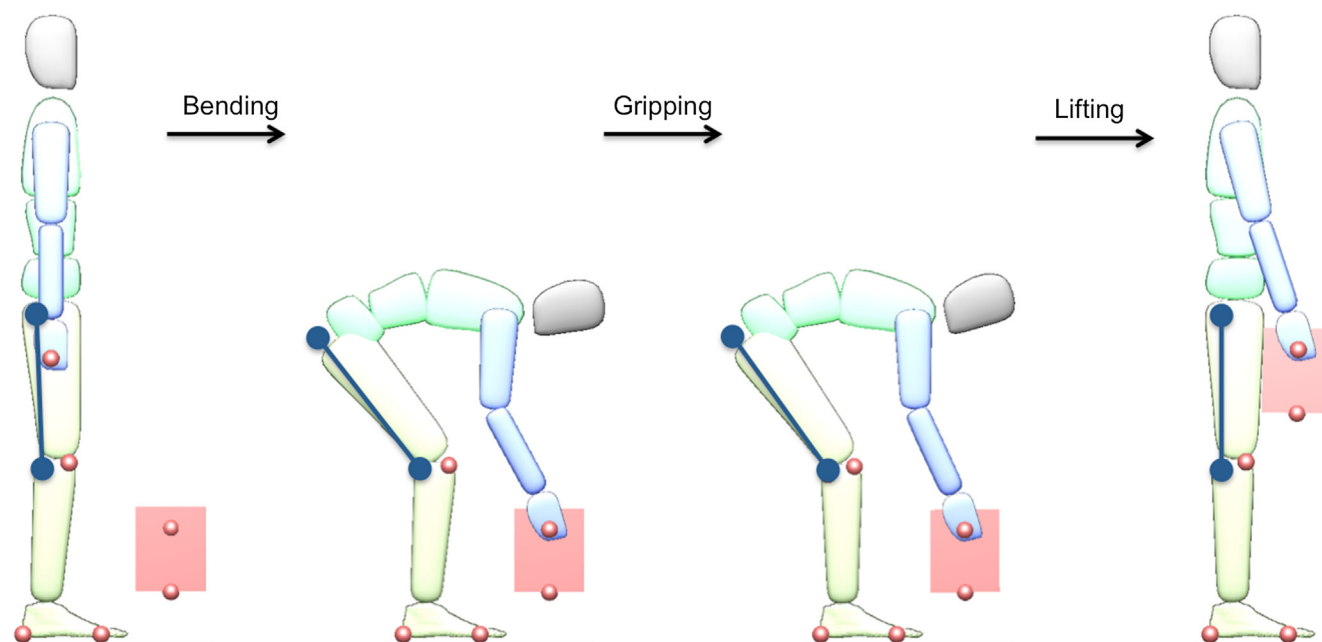| Joints	t_{ad} (ms) [EMD (ms)]	
	Extension MTG	Flexion MTG
Hip	132 [110]	52 [50]
	(Blackburn et al., 2009)	(Begovic et al., 2014)
Knee	52 [50]	132 [110]
	(Begovic et al., 2014)	(Blackburn et al., 2009)
Ankle	46 [45]	149 [120]
	(Winter and Brookes, 1991)	(Úbeda et al., 2017)
Lumbar	169 [130]	251 [160]
	(van Dieën et al., 1991)	(Thelen et al., 1994)

Fig. 2. Motion phases of the optimal control problem. The three motion phases delineate the changing constraints on the multi-body system, which also changes the underlying dynamics.

2. *Gripping* - At the start of the gripping phase, the position of the point on the hand segment (corresponding to the distal second metacarpal) was constrained to match the grip point of the box 0.3 m off the ground. The hand translational and rotational velocities as well as hand forces were set to zero at the start of gripping.

3. *Lifting* - At the start of the lifting phase the vertical hand force was constrained to be equal to the force required to support the weight of the box. The box and hand were affixed together in this phase using 3 kinematic constraints. The end of this phase constrained the human model to stand upright and still.

Additional constraints were active through all phases.

1. We maintained the model's balance by constraining the vertical foot contact forces to be strictly positive.
2. The ratio of horizontal to vertical contact forces were constrained to not exceed a coefficient of friction of 0.8.
3. The two trunk segments were constrained to move together at the same angular velocities.

The bending and lifting phase durations were variables of the OCP. The gripping phase duration was fixed to 0.125 s based on experimental observations of the time required by subjects to grip and lift a box off the ground (Harant et al., 2017).

2.3. Experimental comparisons

We compare our predictions to experimental data recorded as part of a previous study (Harant et al., 2017). We recorded full body kinematics, ground reaction forces, and hand-box forces of 4 male subjects (age 21–25 years, weight 67–103 kg, height 1.7–

1.9 m) lifting a 10 kg box using a stoop lift. Joint angle trajectories were computed from marker positions using least-squares optimization. Joint torques were computed from joint angles, recorded ground reaction forces, and recorded hand-box forces using inverse dynamics analysis. Further detail about the experimental analysis is available in Harant et al. (2017). In addition, we report the values for lumbar flexion and lumbar net torque from Kingma et al. (2004) and Faber et al. (2011). The values reported from Kingma et al. are the average and standard deviation across 10 subjects, using a stoop lift to pick up a 10.5 kg box from a height of 0.5 m above the ground. Faber et al. reported results from 9 subjects lifting a 16.8 kg box from a height of 0.32 m above the ground.

3. Results

The predicted joint angles and net joint torques of the average-lifter match the experimental observations for most of the joints (Fig. 3). The peak hip, knee and lumbar angles were within 1 s.d. of the average subject from Harant et al. (2017). The peak lumbar angle was very close to the average value reported by Kingma et al. (2004) and close to the +1 s.d. range of that reported by Faber et al. (2011). Table 3 lists and compares the results from the average-lifter to the experimental results from Harant et al. (2017).

Modifying the hip and lumbar flexibility produced marked changes in the joint kinematics (Fig. 3a–c). For each of the lifters, the peak lumbar flexion reached the limit imposed on that model type (dashed lines in Fig. 3c). The reduced flexibility at the hip was overcome by bending the knee, thus relaxing the hamstring muscle and allowing the hip to flex beyond what is possible with a straight-knee (dashed lines in Fig. 3a). As the model was made
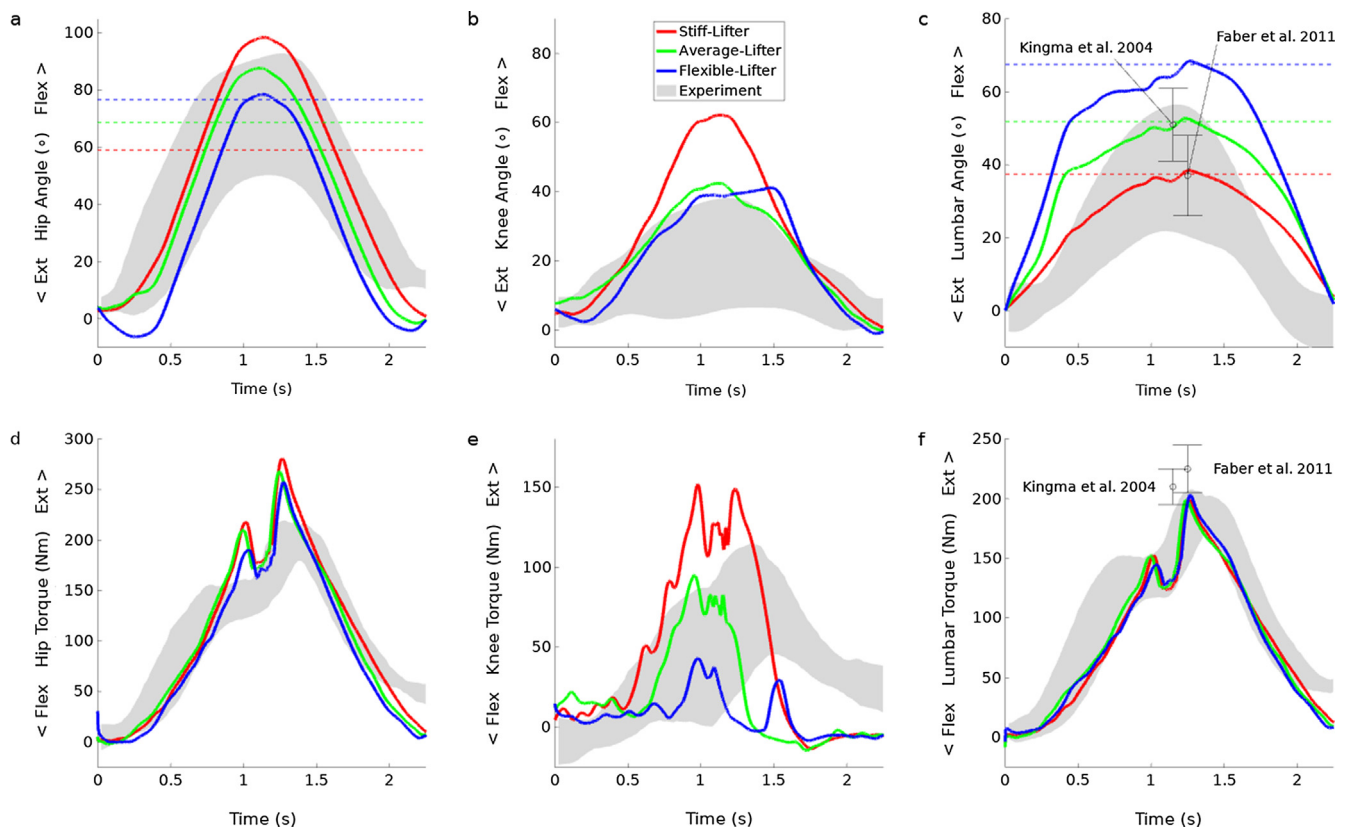

Fig. 3. Joint angles at the (a) hip, (b) knee and (c) lumbar joints. Dashed lines in panes (a) and (c) indicate the flexion limits for stiff, average and flexible humans. Note that the indicated hip flexion limit (panel (a)) is with a straight-knee. Panels (d), (e) and (f) show the net torques at the hip, knee and lumbar joints, respectively. Shaded regions indicate standard deviation from experimental recordings, scaled to the average model motion duration (Harant et al., 2017).

Table 3
Comparison of average-lifter (green lines in Fig. 3) joint angles and joint torques to experimental results from Harant et al. (2017). Reported are the root mean square (RMS) differences between the average-lifter and the average experimental results, the maximum distance between the average-lifter and the experimental envelope, and the maximum experimental variation for comparison. Note that the lumbar angle reported here is the summation over the two trunk segments of our model.

		Hip Joint	Knee Joint	Lumbar Joint
Joint angles	RMS Average-Lifter vs. Exp. Average	13.4°	14.0°	19.9°
	Max. distance Average-Lifter vs. Exp. Range	12.6°	4.2°	21.7°
	Max. Exp. Variation	26.2°	16.4°	17.9°
Joint torques	RMS Average-Lifter vs. Exp. Average	28.3 Nm	37.1 Nm	17.5 Nm
	Max. distance Average-Lifter vs. Exp. Range	53.7 Nm	49.0 Nm	28.1 Nm
	Max. Exp. Variation	40.5 Nm	47.3 Nm	43.2 Nm

more flexible, the optimal solution is one that favors more lumbar flexion and less hip flexion. This can be observed at the point of lifting by comparison of the model pose (Fig. 5). We observed an absolute difference in hip flexion of 11.2° and 9.6° between the stiff and average lifters, and the flexible and average lifters respectively. The corresponding differences in lumbar flexion were 14.2° and 15.5°.

Peak net joint torque at the hip joint (Fig. 3d) increased as the model was made more flexible. Peak net lumbar joint torque

(Fig. 3f) and CLBL (area under curves in Fig. 3f) were similar across models. The ratio of peak lumbar/hip angle increased as the model was made more flexible. The peak normalized passive lumbar extension torque was similar across models with values between 14% and 15% (Fig. 4a). Peak normalized passive hamstring forces decreased from 24.3% to 6.9% with increasing model flexibility (Fig. 4b). The models took 2.36, 2.32 and 2.29 s to complete the lift, while the range for the experimental lifts was from 2.72 to 4.32 s. Table 4 lists and compares the result values across the 3 model types.

4. Discussion

We have presented results from a human model simulation of lifting a box and the variation of the model motion as a function of hip and lumbar flexibility. In general, the lifting motion corresponding to an average person's model matched results from literature (Kingma et al., 2004; Faber et al., 2011) (Fig. 3) and experimental recordings from Harant et al. (2017). There were however exceptions to this trend; when compared to the average lumbar flexion angle from Harant et al. (2017), the results from the stiff-lifter were a closer match than the average-lifter. This could be because the subjects tested in Harant et al. (2017) were as a group close to the stiff case. We also note that the results from Faber et al. (2011) were close to the stiff-lifter in the present study, and in general there appears to be a large variation in lumbar flexion angles reported in the literature (for equivalent lifting tasks). A marked difference was found in the profile of the predicted lumbar angle during the bending and lifting phases, when compared to the experimental range (green line in Fig. 3c). We speculate that these differences could be due to an underestimation of muscle damping in the model, and/or, due to the time-constants used in the activation dynamics not fitting the subjects very well. To improve the fit of the lumbar angle profiles, it may be interesting to treat the damping parameter and activation time constant as free parameters of an optimization problem.

The peak net hip torques in the model were higher than those in the experimental range (Fig. 3d). The speed of the motion can have a strong influence on the peak joint torques. Our model simulations typically completed the motion slightly faster than the average observed across subjects, and this was likely the cause for the higher torques. A solution could be to include additional terms in the cost function that penalize fast motions. Another difference between model and experimental results, was found in the torques about the knee joint Fig. 3e. While the peak torque at the knee matched the experimental range, the torque profile during the lifting phase was underestimated. It is possible that the suggested changes in muscle damping, activation time-constants and penalization of fast motions, may also improve the profile of knee torques.

The changes in the model's motion characteristics as a function of flexibility provided some interesting insights into possible lifting strategies. The stiff-lifter had the highest knee flexion and hip
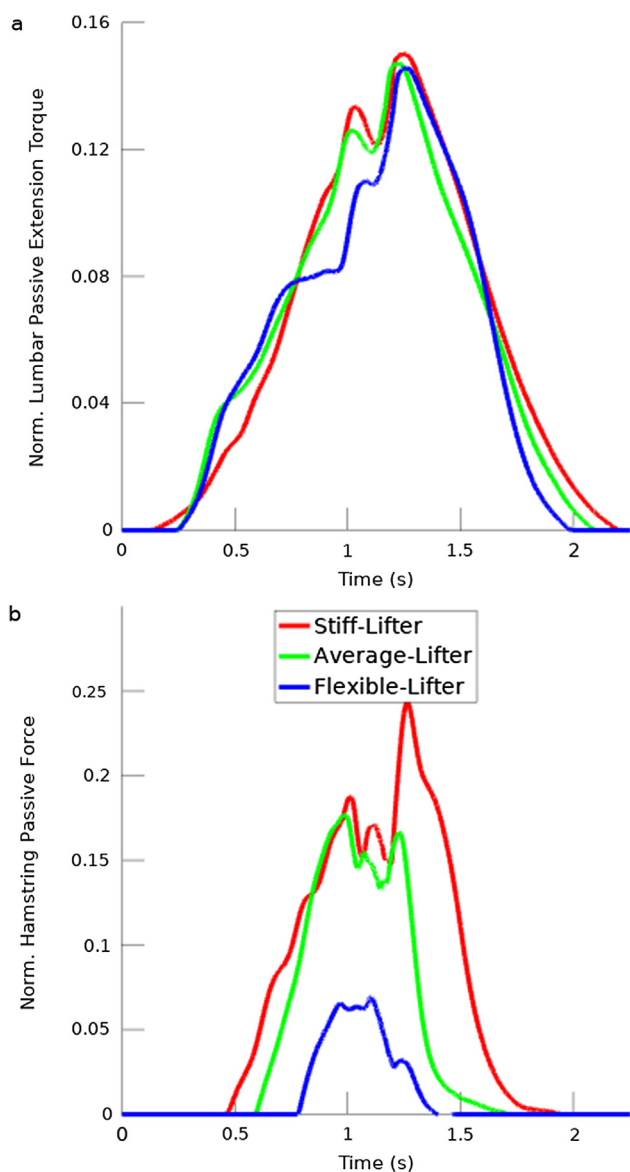
Fig. 4. Comparison of (a) normalized passive lumbar extensor torque, and (b) normalized passive hamstring force for the three lifter models.
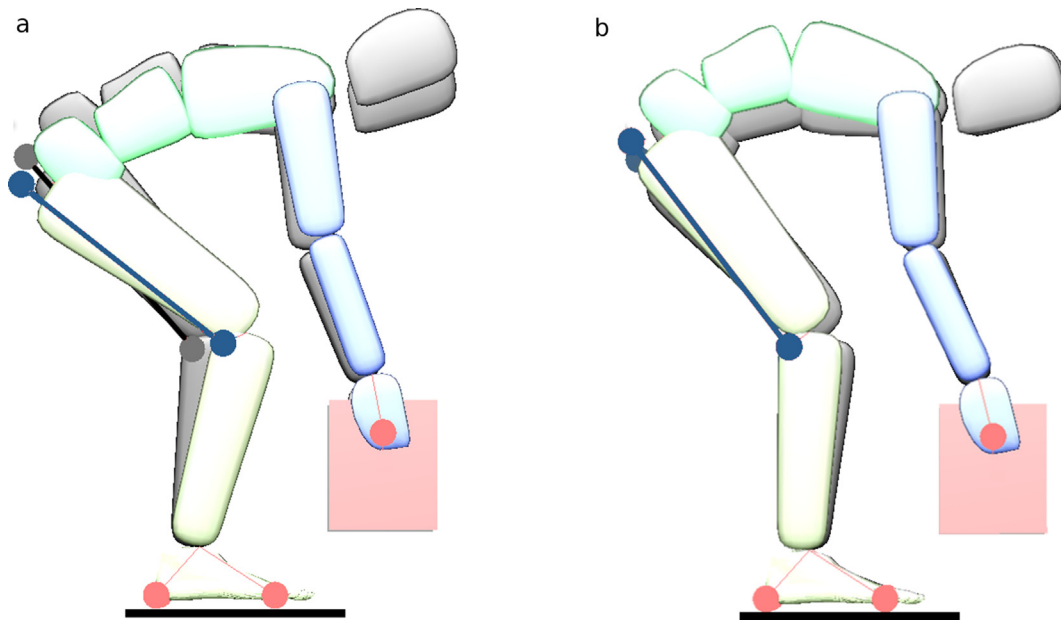
Fig. 5. Comparison of model pose at start of lifting phase. (a) Stiff vs. average-lifter (b) Flexible vs. average-lifter. In both panels, the average-lifter is colored in gray in the background.

Table 4
Comparison of torque and force characteristics for the stiff, average and flexible-lifters. Positive net torques indicate extension torques at the hip and lumbar joints.

	Stiff-Lifter	Average-Lifter	Flexible-Lifter
Norm. Lumbar MTG Passive Extension Torque	15.0%	14.7%	14.5%
Norm. Hamstring Muscle Passive Force	24.3%	17.7%	6.9%
Peak Net Hip Joint Torque	216.2 Nm	226.2Nm	250.0Nm
Peak Net Lumbar Joint Torque	198.9 Nm	198.9 Nm	203.0 Nm
Cumulative Lower Back Load (CLBL)	185.7 Nm s	189.8 Nm s	184.5 Nm s
Ratio Peak Lumbar/Hip Angle	0.39	0.60	0.87

flexion, thus allowing the hamstring muscle to relax, while having the lowest lumbar flexion. In comparison the average and flexible-lifters used less hip and knee flexion and more lumbar flexion. Studies have reported similar increases in lumbar flexion with increased flexibility of the hamstring muscle due to stretching exercise (Kang et al., 2013), and due to repeated lifts that increase flexibility (Dolan and Adams, 1998). Our simulations suggest that the different contributions of passive forces for the three lifters played a major role in the coordination of the limbs during lifting (Fig. 4). The additional passive components with increasing model stiffness, and the associated penalty in the OCP were the likely reason behind the differences in lifting styles. Interestingly, the magnitudes of the normalized passive forces/torques were similar across models for the lumbar back but not for the hamstring muscle. It is however unclear if this trend extends to real world lifting, as it may also be possible that a person is more tolerant of passive forces in the hamstring rather than at the lumbar back (or vice versa), in which case the cost function used to simulate that person's lifting style would have to be appropriately weighted. Additionally, our cost function formulation equally weights the active and passive muscle components, as well as the relative weighting between MTGs. It is possible that these weights vary between joints, active and passive components and additionally between individuals and tasks. Deducing subject-specific and task-specific

weights is an important and difficult problem. A possible solution here could be the use of inverse optimal control (Mombaur, 2016; Clever et al., 2016) that can be used to identify specific optimization criteria from recorded experimental data.

The plausibility of the predicted pattern was supported by results from studies on gender based differences in lifting technique. Lumbar flexion angle in men has been found to be larger than that of women (Sullivan et al., 1994). Thomas et al. concluded that ROM and lifting technique may be contributing factors towards observed differences between the motion kinematics of male and female subjects (Thomas et al., 1998). They also reported that men flex equally at the hip and spine, whereas women use minimal spine flexion. In our simulations, we observed a similar trend as (Thomas et al., 1998), with the ratio of peak lumbar/hip angle increasing with model flexibility.

The strong influence of model stiffness on optimal lifting motions raises some interesting perspectives towards the design of assistive devices (exoskeletons) such as the Laevo V2 (Laevo NL) and backX (US Bionics). Exoskeletons that provide lifting assistance using passive spring-like elements work in parallel with the body and can change the effective stiffness at the hip and lumbar joints. Our findings suggest that this could in turn result in changes in the motion, the passive muscle forces/joint torques, as well as the cumulative lower back load. These changes have implications for the design of the exoskeleton from a user-safety point of view, and as well, for predicting how effective the exoskeleton would be at reducing overall effort. In order to maximize assistance while minimizing the change from a person's natural motion, it may be necessary to make a careful choice of exoskeleton hip and lumbar spring stiffness and to take into account the variation in flexibility between users.

The model used in this study was relatively simple and did not contain more detailed aspects that affect joint loading such as multijoint equilibrium and translational DOF in the spine (Dreischarf et al., 2016). The trade-off here was to have a computationally tractable problem that simulates motion of the whole body, including the lower limbs, arms, and as well the interaction with the environment (ground reaction forces and hand-box forces). Additionally, the segment lengths, masses, inertias etc were built by

scaling from average properties reported in literature (e.g. (de Leva, 1996)) which may not be close to the average of the subject populations used for comparison. We also note that in this study we have only varied some of the aspects that could potentially contribute towards a person's lifting technique. Additional factors such as relative muscle strength, anatomical differences and task-specific requirements may play just as important a role in deciding motion characteristics. In order to establish the validity of our simulation results we additionally need to compare to similarly grouped populations of stiff, average and flexible persons (for example in a manner similar to the study design followed by Gajdosik et al. (1994)).

Conflict of interest statement

The Authors declare that there were no conflicts of interest related to this work.

Acknowledgments

Appendix A. Supplementary material

Supplementary data associated with this article can be found, in the online version, at https://doi.org/10.1016/j.jbiomech.2018.07.028.

References

Ackermann, M., van den Bogert, A., 2010. Optimality principles for model-based prediction of human gait. J. Biomech. 43 (6), 1055–1060.

Afschrift, M., Jonkers, I., Schutter, J.D., Groote, F.D., 2016. Mechanical effort predicts the selection of ankle over hip strategies in nonstepping postural responses. J. Neurophysiol. 116 (4), 1937–1945.

Anderson, F., Pandy, M., 2001. Dynamic optimization of human walking. ASME J. Biomech. Eng. 123 (5), :381–390.

Arjmand, N., Shirazi-Adl, A., 2006. Sensitivity of kinematics-based model predictions to optimization criteria in static lifting tasks. Med. Eng. Phys. 28 (6), 504–514.

Begovic, H., Zhou, G.-Q., Li, T., Wang, Y., Zheng, Y.-P., 2014. Detection of the electromechanical delay and its components during voluntary isometric contraction of the quadriceps femoris muscle. Front. Physiol. 5, 494.

Blackburn, J.T., Bell, D.R., Norcross, M.F., Hudson, J.D., Engstrom, L.A., 2009. Comparison of hamstring neuromechanical properties between healthy males and females and the influence of musculotendinous stiffness. J. Electromyogr. Kinesiol. 19, e362–369.

Bock, H.G., Pitt, K.J., 1984. A multiple shooting algorithm for direct solution of optimal control problems. In: 9th IFAC World Congress Budapest.

Brand, R.A., Crowninshield, R.D., Wittstock, C.E., Pederson, D.R., Clark, C.R., van Kricken, F.M., 1982. A model of lower extremity muscular anatomy. J. Biomech. Eng. 104, 304–310.

Burg, J.v.d., Casius, L., Kingma, I., Dieën, J.v., Soest, A.v., 2005. Factors underlying the perturbation resistance of the trunk in the first part of a lifting movement. Biol. Cybern. 93 (1), 54–62.

Buseck, M., Schipplein, O.D., Andersson, G.B.J., Andriachhi, T.P., 1987. Influence of dynamic factors and external loads on the moment at the lumbar spine in lifting. Spine (Phila Pa) 13 (8), 918–921.

Christophy, M., Senan, N.A.F., Lotz, J.C., O'Reilly, O.M., 2012. A musculoskeletal model for the lumbar spine. Biomech. Model. Mechanobiol. 11 (1–2), 19–34.

Clever, D., Schemschat, R.M., Felis, M.L., Mombaur, K., 2016. Inverse optimal control based identification of optimality criteria in whole-body human walking on level ground. In: 2016 6th IEEE International Conference on Biomedical Robotics and Biomechatronics (BioRob), pp. 1192–1199.

Coenen, P., Kingma, I., Boot, C., Twisk, J., Bongers, P., van Dieën, J., 2013. Cumulative low back load at work as a risk factor for low back pain: a prospective cohort study. J. Occupat. Rehabil. 23 (1), 11–18.

de Leva, P., 1996. Adjustments to Zatsiorsky-Seluyanov's segment inertia parameters. J. Biomech. 29 (9), 1223–1230.

Dolan, P., Adams, M., 1998. Repetitive lifting tasks fatigue the back muscles and increase the bending moment acting on the lumbar spine. J. Biomech. 31 (8), 713–721.

Dolan, P., Mannion, A., Adams, M., 1994. Passive tissues help the back muscles to generate extensor moments during lifting. J. Biomech. 27 (8), 1077–1085.

Dreischarf, M., Shirazi-Adl, A., Arjmand, N., Rohlmann, A., Schmidt, H., 2016. Estimation of loads on human lumbar spine: a review of in vivo and computational model studies. J. Biomech. 49 (6), 833–845. SI: Spine Loading and Deformation.

Faber, G.S., Kingma, I., van Dieën, J.H., 2011. Effect of initial horizontal object position on peak l5/s1 moments in manual lifting is dependent on task type and familiarity with alternative lifting strategies. Ergonomics 54 (1), 72–81.

Gajdosik, R.L., Albert, C.R., Mitman, J.J., 1994. Influence of hamstring length on the standing position and flexion range of motion of the pelvic angle, lumbar angle, and thoracic angle. J. Orthop. Sports Phys. Therapy 20 (4), 213–219.

Harant, M., Sreenivasa, M., Millard, M., Sarabon, N., Mombaur, K., 2017. Parameter optimization for passive spinal exoskeletons based on experimental data and optimal control. In: Proceedings of the 2017 IEEE-RAS International Conference on Humanoid Robots.

Hoy, M.G., Zajac, F.E., Gordon, M.E., 1990. A musculoskeletal model of the human lower extremity: the effect of muscle, tendon, and moment arm on the moment-angle relationship of musculotendon actuators at the hip, knee and ankle. J. Biomech. 23 (2), 157–169.

Kang, M.-H., Jung, D.-H., An, D.-H., Yoo, W.-G., Oh, J.-S., 2013. Acute effects of hamstring-stretching exercises on the kinematics of the lumbar spine and hip during stoop lifting. J. Back Musculoskeletal Rehabil. 26 (3), 329–336.

Kingma, I., Bosch, T., Bruins, L., van Dieën, J.H., 2004. Foot positioning instruction, initial vertical load position and lifting technique: effects on low back loading. Ergonomics 47 (13), 1364–1385.

Leineweber, D.B., Bauer, I., Bock, H.G., Schlöder, J.P., 2003. An efficient multiple shooting based reduced SQP strategy for large-scale dynamic process optimization. Part 1: Theoretical aspects. Comput. Chem. Eng. 27 (2), 157–166.

Manns, P., Sreenivasa, M., Millard, M., Mombaur, K., 2017. Motion optimization and parameter identification for a human and lower back exoskeleton model. IEEE Robot. Automat. Lett. 2 (3), 1564–1570.

Millard, M., Sreenivasa, M., Mombaur, K., 2017. Predicting the motions and forces of wearable robotic systems using optimal control. Front. Robot. AI 4, 41.

Millard, M., Uchida, T., Seth, A., Delp, S.L., 2013. Flexing computational muscle: modeling and simulation of musculotendon dynamics. ASME J. Biomech. Eng. 135 (2).

Mombaur, K., 2016. Optimal Control for Applications in Medical and Rehabilitation Technology: Challenges and Solutions. Springer International Publishing, Cham, pp. 103–145.

Mombaur, K., Hoang, K.-L.H., 2017. How to best support sit to stand transfers of geriatric patients: Motion optimization under external forces for the design of physical assistive devices. J. Biomech. 58, 131–138.

Sadeghi, M., Andani, M.E., Bahrami, F., Parnianpour, M., 2013. Trajectory of human movement during sit to stand: a new modeling approach based on movement decomposition and multi-phase cost function. Exp. Brain Res. 229, 221–234.

Serrancolí, G., De Schutter, J., De Groote, F., 2017. Analysis of Optimal Control Problem Formulations in Skeletal Movement Predictions. Springer International Publishing, Cham, pp. 1269–1273.

Solomonow, M., Baratta, R., Zhou, B.-H., Burger, E., Zieske, A., Gedalia, A., 2003. Muscular dysfunction elicited by creep of lumbar viscoelastic tissue. J. Electromyogr. Kinesiol. 13 (4), 381–396.

Sreenivasa, M., Harant, M., 2018. Modelfactory: A matlab/octave based toolbox to create human body models. CoRR, abs/1804.03407.

Sreenivasa, M., Millard, M., Felis, M., Mombaur, K., Wolf, S.I., 2017. Optimal control based stiffness identification of an ankle-foot orthosis using a predictive walking model. Front. Comput. Neurosci. 11, 23.

Steele, K.M., van der Krogt, M.M., Schwartz, M.H., Delp, S.L., 2012. How much muscle strength is required to walk in a crouch gait? J. Biomech. 45 (15), :2564–2569.

Sullivan, M.S., Dickinson, C.E., Troup, J.D., 1994. The influence of age and gender on lumbar spine sagittal plane range of motion. a study of 1126 healthy subjects. Spine (Phila Pa 1976) 19 (6), 682–686.

Thelen, D.G., 2003. Adjustment of muscle mechanics model parameters to simulate dynamic contractions in older adults. Trans. ASME 125, 70–77.

Thelen, D.G., Schultz, A.B., Ashton-Miller, J.A., 1994. Quantitative interpretation of lumbar muscle myoelectric signals during rapid cyclic attempted trunk flexions and extensions. J. Biomech. 27 (2), 157–167.

Thomas, J.S., Corcos, D.M., Hasan, Z., 1998. The influence of gender on spine, hip, knee, and ankle motions during a reaching task. J. Mot. Behav. 30 (2), 98–103.

Úbeda, A., Vecchio, A.D., Sartori, M., Puente, S.T., Torres, F., Azorín, J.M., Farina, D., 2017. Electromechanical delay in the tibialis anterior muscle during time-varying ankle dorsiflexion. In: 2017 International Conference on Rehabilitation Robotics (ICORR), pp. 68–71.

van Dieën, J.H., Kingma, I., 2005. Effects of antagonistic co-contraction on differences between electromyography based and optimization based estimates of spinal forces. Ergonomics 48 (4), 411–426.

van Dieën, J.H., Thissen, C.E.A.M., van de Ven, A.J.G.M., Toussaint, H.M., 1991. The electro-mechanical delay of the erector spinae muscle: influence of rate of force development, fatigue and electrode location. Eur. J. Appl. Physiol. 63 (3-4), 216–222.

Winter, E.M., Brookes, F.B., 1991. Electromechanical response times and muscle elasticity in men and women. Eur. J. Appl. Physiol. 63 (2), 124–128.